Mild, Additive-Free Thioetherification via Proton Transfer Dual Ionization Mechanism

Christian R. Zwick III*, Jeremy J. Henle, Shashank Shekhar, Cassie Yang, Yong Zhou, Amanda L. Wall, Rodger F. Henry

Address: AbbVie Process Research & Development, 1401 N. Sheridan Road, North Chicago, Illinois 60064, United States
Keywords: *thioetherification, thiol, proton transfer dual ionization, nucleophilic aromatic substitution, photochemistry, C-S coupling, reaction progress kinetic analysis, rate-limiting proton transfer, DRF calculations*

ABSTRACT: Thioethers represent prevalent motifs in highly sought after biologically active small molecules such as active pharmaceutical ingredients (APIs) and natural products. While nucleophilic aromatic substitution (S_NAr) has traditionally been used to synthesize aryl thioethers, modern approaches leverage transition metals to catalyze thermal or photochemical cross-coupling. During platform technology development for photochemical transformations, we uncovered an exceedingly mild thioetherification that does not require light, transition metal or exogenous base. An array of thiols and halogenated heterocycles were coupled to produce 40 diverse products including the penultimate precursor to the immunosuppressant azathioprine (1-step). Reaction progress kinetic analysis (RPKA) and computational studies support a unique mechanism, here termed proton transfer dual ionization (PTDI) S_NAr. Rate-limiting proton transfer (RLPT) pre-equilibrium results in dual nucleophile and electrophile ionization prior to an asynchronous concerted S_NAr. This transformation complements modern approaches to thioethers and motivates additional research evaluating PTDI as a general activation mode between coupling partners.

Introduction

Alkyl and aryl thioethers (sulfides) represent common motifs among active pharmaceutical ingredients (APIs) and natural products such as azathioprine, nolatrexed and the penicillin's (Scheme 1A).[1] This motif is considered privileged in medicinal chemistry based on unique pharmacological properties mediated through NH mimicry, redox non-innocence (sulfoxide-sulfone interconversion) and intra-/intermolecular carbon-sulfur (C-S) σ* orbital interactions, among others.[1c-e] Given the ubiquity of thioethers in biologically active compounds, numerous 'C-S coupling' strategies have been reported.[2] Traditionally, thioethers are synthesized from thiols and electron deficient aryl halides using strong bases, polar solvents, and high temperatures via nucleophilic aromatic substitution (S_NAr) (Scheme 1B).[2a-c] State-of-the-art coupling involves transition metal (TM) catalysts (Pd, Ni) that display broader scope but usually at higher cost (Scheme 1B).[2d,e] Recent photochemical innovations provide ambient temperature alternatives to S_NAr and TM catalyzed approaches to thioethers (Scheme 1B).[2d,e] Although most reports utilize photoredox (Ir or Cu, hν) or metallaphotoredox (Ru or Ir w/ Ni, hν) catalysis, one noteworthy exception requires no photocatalyst (PC) (White LED, Cs_2CO_3, DMSO) (Scheme 1C).[2e,f] Developed by Miyake and co-workers, this reaction proceeds through a unique mechanism involving intermolecular charge transfer (CT) via a thiolate-aryl halide electron donor-acceptor (EDC) complex prior to C-S bond formation. Perhaps more impressive is the reaction's general utility, low cost and simple setup. In our continued effort to implement photochemical transformations in pharmaceutical process development, we became motived to implement these conditions.[3] Through this endeavor, a light, transition metal and exogenous base free thioetherification was discovered (Scheme 1D). A diverse array of functional group rich thiols and halogenated heterocycles could be coupled under exceedingly mild conditions.[2j] Finally, a unique mechanism was identified, here termed proton transfer dual ionization (PTDI) S_NAr, which enables the simple and mild nature of the transformation.

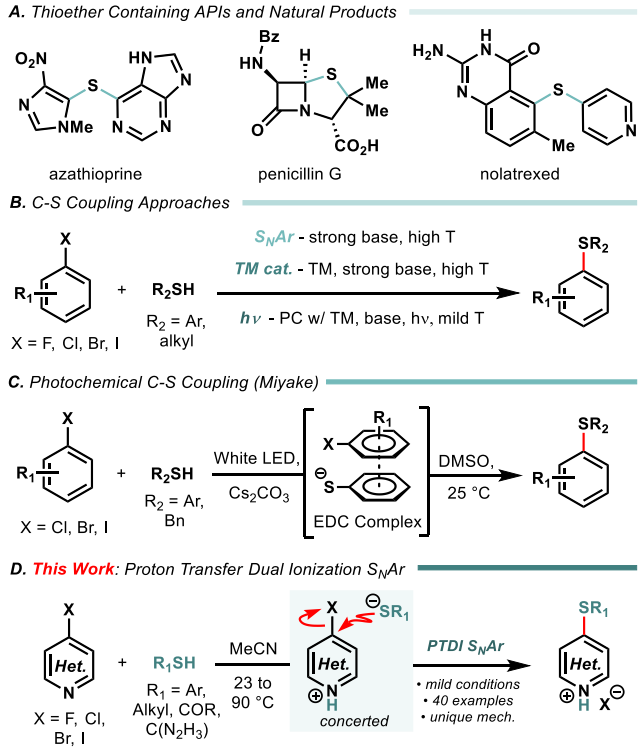

Scheme 1. A. Thioether containing molecules. **B.** Synthetic approaches to aryl thioethers. **C.** Photochemical C-S coupling reported by Miyake and co-workers. **D.** Proton Transfer Dual Ionization (PTDI) S_NAr.

Results and Discussion

To begin our development, sodium 5-chloropyrazine-2-thiolate (**1a**) and 5-fluoro-4-iodopyridin-2-amine (**2a**) were selected from our building block library to stress the robustness of Miyake's reported conditions.[4,5] **1a** and **2a** are challenging substrates that contain nucleophilic and electrophilic functionality capable of cross and self-coupling photochemically or thermally (S_NAr).[2a,6] **1a** and **2a** were additionally selected based on the ubiquity of nitrogen containing heterocycles in small-molecule drugs and their propensity to complicate TM catalyzed cross-coupling reactions.[7] Submitting **1a** and **2a** to 450 nm irradiation in DMSO at 40°C (Table 1, Entry 1) generated **3a** (15%) as a complex mixture with several by-products (23%) and unreacted **2a** (62%). **4** was identified as the largest by-product (5%), likely formed from over-reaction of **3a** with **1a**. The remaining by-products (18%) are suspected to be oligomers derived from **1a** based on its consumption relative to **2a** and the formation of **4**. Switching from DMSO to MeCN gave an improvement in conversion to **3a** (26%) but an increase in **4** (10%) (Table 1, Entry 2). To probe if S_NAr was a dominant pathway these conditions were repeated in the absence of light resulting in trace product and by-product formation (Table 1, Entry 3). Given **1a**'s complete consumption, we posited that evaluating various solvents and soluble organic bases with thiophenol **1b** might taper the thiolate's reactivity thus reducing by-product formation. While stronger bases like NEt_3 (pKa = 9.0, DMSO) gave minimal conversion to **3a** (8%) (Table 1, Entry 4), the weak base pyridine (pKa = 3.4, DMSO) (Table 1, Entry 5) resulted in 85% conversion.[8] This significant improvement can be partly attributed to **1b**'s limited solubility, a consequence of pyridine's reduced propensity to generate the soluble thiolate anion, resulting in improved chemoselectivity because of inefficient mass transfer.[9] Additionally, **2a**'s complete consumption may be explained by N-activation (e.g. H-bond, PCET, PT) which was likely inhibited by strong base under the previous conditions tested.[9,10] N-activation of basic heterocycles such as pyridine are ubiquitous, boding favorably for this hypothesis (*vida infra*).[2b,10,11] While Entry 5 afforded excellent conversion, **4** was still generated in undesirable quantities (6%). Tapering **3a**'s solubility was hypothesized to reduce **4**, since switching from MeCN to PhMe gave minimal conversion (17%) but only trace **4** (Table 1, Entry 6). In turn, various solvents were evaluated in the absence of pyridine in hope of eliminating **4** and to test if **2a** was undergoing proton transfer. Balancing solvent polarity proved critical since PhMe (Table 1, Entry 7) gave almost no conversion while DMSO (Table 1, Entry 8) gave significant formation of disulfide **5** (11%) from **1b**. MeCN (Table 1, Entry 9) worked best, giving **3a** in high conversion with only trace **4** and **5**. The absence of exogenous base and low organic solubility allowed **3a** to precipitate from the reaction as an HI salt (**3b**) which could then be collected through filtration in high yield and purity (91% yield, Scheme 3 *vide infra*).

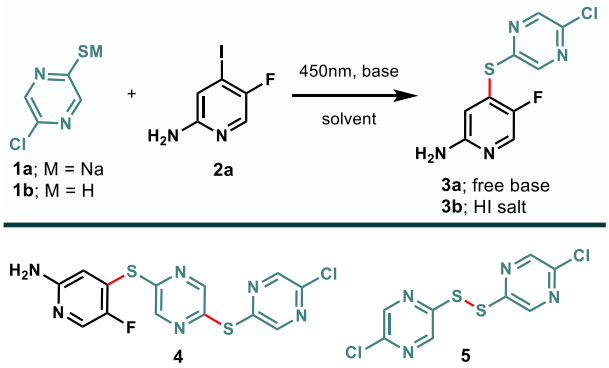

#	Solvent	M	1	2	3	4	5	RA
1	DMSO	Na	<1	62	15	5	<1	18
2	MeCN	Na	12	42	26	10	<1	10
3^	MeCN	Na	41	53	<1	<1	<1	5
4*	MeCN	H	33	43	8	7	<1	9
5⁺	MeCN	H	5	<1	85	6	<1	3
6⁺	PhMe	H	35	37	17	<1	1	10
7	PhMe	H	48	39	5	<1	5	3
8	DMSO	H	<1	9	71	4	11	2
9	MeCN	H	12	5	81	<1	<1	1
10^	MeCN	H	10	4	84	<1	<1	1

Table 1. A. Tabulated numbers are HPLC PA% at 210nm. RA = residual area, *3 equiv NEt_3 added, ⁺3 equiv pyridine added, ^No-light, 91% yield. **B.** General conditions: **1** (0.14 mmol, 1.1 equiv), **2a** (0.11 mmol, 1.0 equiv), solvent (0.2M), 450 nm LED, 40°C, 18h.

As a control, we performed an experiment in the absence of light and were surprised to observe identical performance. This unexpected result suggested a change in

mechanism to Miyake's reported conditions. To gain mechanistic understanding that might guide substrate scope evaluation, we set out to determine key reaction parameters enabling the transformation (Scheme 2). As previously discussed, no product is observed when using **1a** instead of **1b** (Table 2, Entry 1). By contrast, the reaction proceeds with thiolate **1a** when using pyridinium salt **2b** (Table 2, Entry 2), likely generating **2a** and **1b** as the reaction proceeds. Furthermore, using sub stoichiometric quantities of **1b** (1 equiv of a 9:1 mixture of **1a**:**1b**) gave complete conversion (Table 2, Entry 3), supporting **1b** can be reformed from proton transfer between **1a** and **3b**, and that the reaction can be acid catalyzed. Like Table 2, Entry 1, no reaction is observed when combining **1b** and **2b** (Table 2, Entry 4), indicating a basic component is required. Using a thiophenol proved important since switching **1b** (pKa~10, DMSO) to benzyl mercaptan (**6**) (pKa = 15.3, DMSO) shuts off the reaction (Table 2, Entry 5).[12] To probe if electrophile activation occurs, **2a** was swapped for electronically similar 4-iodonitrobenzene (**7**) paired with pyridine as a base (Table 2, Entry 6) resulting in no product formation.[2b,g] In unity, these control experiments support that the reaction requires activation of **2a** via proton transfer before the coupling can take place.

Activation of basic heterocycles through a nitrogen atom is a well precedented strategy to promote reactivity.[10,11] Pyridine activation is the most well documented, with common approaches including N-methylation, N-oxidation, N-coordination (TM, LA, boron, etc), N-protonation, general N-functionalization, and H-bond activation.[2a,g,10,11] To help distinguish between protonation versus H-bonding for our reaction, we performed ^{1}H NMR titration experiments with pyridine and **1b**. (Figure S2).[10a,b,d] Our results show an absence of discrete downfield peak shifts for pyridine when 1 equivalent of **1b** was reached. Instead, pyridine experienced gradual downfield peak shifting (0.015-0.04 ppm) as the equivalents of **1b** increased. These data advocate for a small proton transfer equilibrium as opposed to formation of a H-bound intermediate in our parent reaction.

We next set out to probe if the reaction mechanism involves electron transfer (ET) akin to a radical-nucleophilic aromatic substitution ($S_{RN}1$) (Table 2, Entries 7-9).[13a] Examples of thermal or light-initiated ET reactions between substrates of similar oxidation potential are rare but known. Running the reaction with 3-iodopyridine (**8**), a suitable substrate for radical coupling, showed no reaction (Table 2, Entry 7).[13b] Additionally, 4-fluoro-2-aminopyridine (**9**), a poor substrate for radical coupling, yielded product (Table 2, Entry 8). Finally, adding a radical trap (TEMPO) didn't capture any intermediates (Table 2, Entry 9).[13c] Taken together these data support a 2-electron mechanism likely akin to S_NAr.

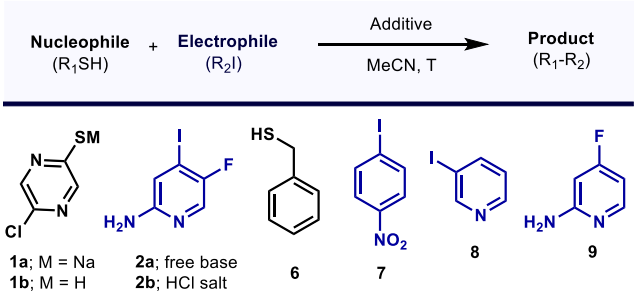

#	Nu	E+	T	Add.	Results
1	1a	2a	40	-	X
2	1a	2b	40	-	√
3	1a:1b (9:1)	2a	40	-	√
4	1b	2b	40	-	X
5	6	2a	70	-	X
6	1b	7	70	pyridine	X
7	1b	8	70	-	X
8	1b	9	23	-	√
9	1b	2a	23	TEMPO	√

Table 2. A. Control experiments elucidating key reaction parameters and general mechanistic features. Nu = nucleophile, E+ = electrophile, PD = product, T = temperature in °C, Add. = additive, N.R. = no reaction, C.C. = complete conversion to product. **B.** General conditions: **Nu** (0.14 mmol, 1.1 equiv), **E+** (0.11 mmol, 1.0 equiv), MeCN (0.2M), 18h.

Classical S_NAr involves the use of a strong base to ionize the nucleophilic component (nucleophile ionization) prior to a rate-determining addition step (RDS), generating a Meisenheimer complex prior to elimination (Scheme S2).[2a-c] Nucleophile ionization is common for less acidic nucleophiles like thiols, alcohols and carbon-based nucleophiles. A less common S_NAr variant involves using Lewis or Brønsted acid to ionize basic electrophiles (electrophile ionization) for coupling with weakly acidic nucleophiles such as anilines, azoles, and amines (Scheme S2).[11a,14] Our control experiments support a hybrid mechanism, where proton transfer ionizes **1b** and **2a** prior to coupling (Scheme 5, *vide infra*). Examples of similar reactions of functionalized pyridines with sulfinic acid or thiophenols have been previously reported, although requiring high temperatures (~100°C), good leaving groups (Cl, pyridyl) and lacking mechanistic understanding.[10c,15] In this case, dual ionization of the electrophile and nucleophile allow for a remarkably mild and chemoselective transformation.

Armed with a preliminary understanding of the reaction requirements and mechanism from our control experiments, we next leveraged this information to guide substrate scope evaluation. We first tested a range of thiophenol nucleophiles with 4-iodopyridine (**10**), which was selected based on its intermediate reactivity (iodide LG, no substituents) and availability as a free base (Table 2). In our hands, electronically rich thiophenols were prone to forming disulfides, prompting coupling of their sodium thiolate salts with 4-bromopyridinium chloride to diminish this side reaction. For purification, the reactions were either filtered directly or submitted to basic work-up followed by column chromatography if needed. This reaction displayed

excellent yields for electronically neutral or sterically encumbered substrates ranging benzenethiol (88%) to 2,6-dimethylthiophenol (87%) (**11**-**14**), albeit requiring mild heating with the latter. Electronically rich thiophenols like 4-methoxythiophenol gave analogous yields (**17**, 88%) while members containing reactive functionality (**15** & **16**, 4-OH, 4-NH_2) performed modestly (42-56%). Remarkably, electronically deficient thiophenols (4-CO_2Me, 4-NO_2, 4-OCF_3) reacted rapidly often reaching completion within 1h, affording products (**18**, **19** & **21**) in >80% yield. This observation contrasts nucleophile ionization reactivity, which typically favor stronger nucleophiles based on a rate-limiting addition step. In unity, as alluded to previously (Table 2, Entry 5), less acidic alkyl thiols showed no reaction (Scheme S3). Heterocycle containing thiophenols such as **1b** exhibited good yield (**23**, 76%), while 4-thiopyridine and 2-benzoxazolethione gave modest to poor yields (**20** & **22**, 23-48%). Of note, while 4-nitrothiophenol and 2-benzoxazolethione had failed in Miyake's report, our conditions provided a successful (albeit low yielding in the latter case) entry to thioethers of this kind.[2f]

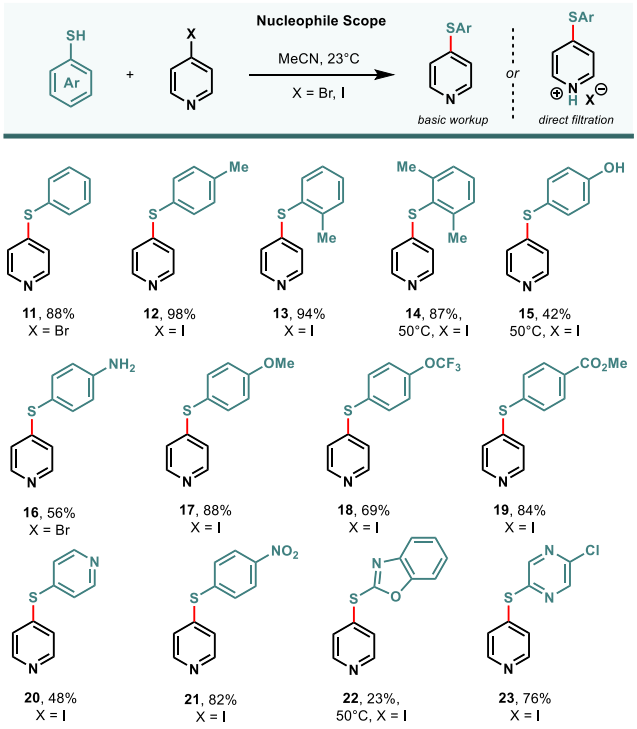

Scheme 2. Thiophenol substrate scope.

For electrophile scope, a variety of different basic halogenated heterocycles were tested with methyl 4-mercaptobenzoate (**24**), which was selected given its superior reactivity and stability compared to other thiophenols (Scheme 3). Akin to **3a**, other 2-amino-4-halopyridines gave high yields (**25**-**28**, 70-96%). By contrast, other halogenation patterns on 2-aminopyridines (3, 5 or 6) gave no reaction (Scheme S4). The halogenated series for 2-amino-4-halopyridine was evaluated, each affording product (**27**) in good to excellent yield (73–99%). Curiously, reaction rate and yield for the series trended F>Br~I>Cl, juxtaposing the standard reactivity trend of F>Cl>Br>I for a traditional nucleophile ionization pathway.[2b,10d] Of note, both acidic (Boc) and basic (ester) functionality, which preclude acid or base mediated S_NAr reactions, were well tolerated under the standard conditions. 2-Iodopyridine also forms product (**31**) but requires higher heating (70°C), likely due to reduced basicity of 2-halogenated pyridines (pKa <2). Related basic halogenated heterocycles (quinolines, naphthyridines and isoquinolines) rapidly form product (**32-34**) in good to great yields (67-87%). By contrast, halogenation on extended pi systems (5-chloroquinoline or 4-bromophenylpyridine) showed no reaction (Scheme S4). For substrates where multiple halogens are present, complete selectivity for a single position was observed uniformly. For imidazopyridines, only the [1,2-α] isomer gave product (**35**) following high heating (61%, 80°C). 2-amino-4/5-bromopyrmidines proved to be excellent substrates producing **36** and **37** in high yield (>90%). By contrast, 2-amino-4-chloropyrazine and 5-bromopyrimidine showed no reaction, while 4-bromopyrimidine gave **38** in only 17% yield. It's worth noting that 5-bromopyrimidine reacts several orders of magnitude more rapidly than 4-bromopyridine under traditional nucleophile ionization S_NAr.[2b] Halogenated azoles such as imidazoles and pyrazoles were unreactive, whereas 2-bromothiazole gave **39** in modest yield (46%) after high heating (90°C) (Scheme S4). Finally, the halogenated nucleotide 6-chloropurine afforded **40** in 85% yield with mild heating (60°C).

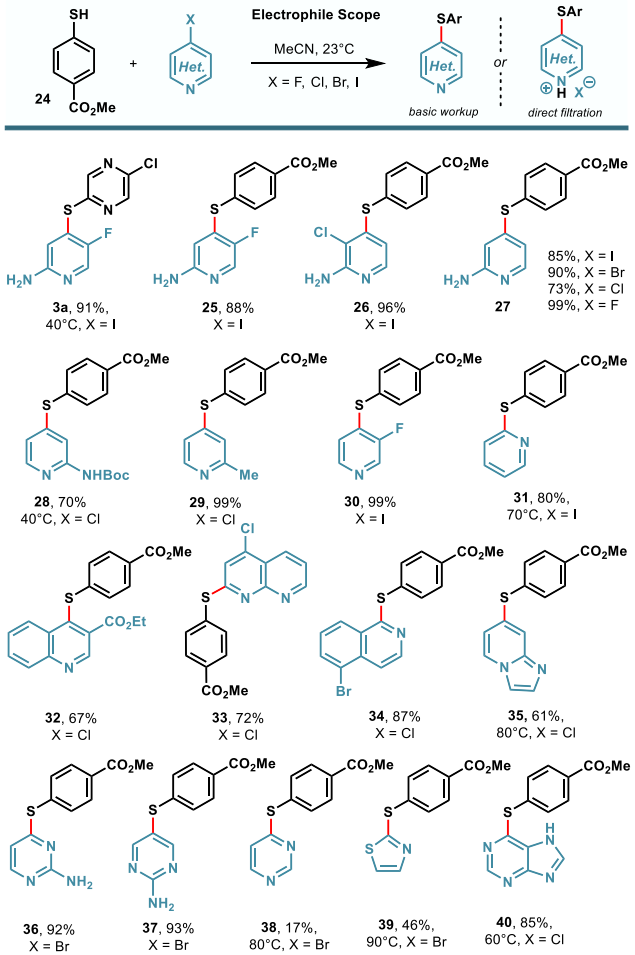

Scheme 3. Halogenated heterocycle substrate scope.

Following our evaluation of various thiophenols and halogenated heterocycles, a handful of thiols and selenols were evaluated (Scheme 4A). Benzeneselenol functioned analogously as benzenethiol producing **41** in 90% yield. Alkyl

thiols generally showed no reaction aside from ethyl glycolate likely due to its increased acidity (pKa ~ 13 vs 17, DMSO).[12b] Thiourea produced **43** in good yield (77%), providing an alternative to TM mediated approaches to arylated thioureas.[16] Finally, thiocarboxylic acids effectively form thioester products. Remarkably, thiobenzoic acid formed thioester **44** in 86% yield, while thioacetic acid produced free thiol **45** in 60% yield. In the latter case, S->N acyl transfer is known and perhaps mediates hydrolysis of the intermediate thioester.[17] This reaction represents a rare traceless thiol installation and provides a valuable alternative to previous approaches using thiol surrogates like the Newman-Kwart rearrangement.[16d,18] To demonstrate the utility of this transformation, thiopurine **46** was synthesized from 6-chloropurine in 92%, representing a 2-step formal total synthesis of the immunosuppressant azathioprine (Scheme 4B).[1a,19]

To gauge distinct reactivity differences between 2 and 4-halopyridines we ran competition experiments between 2-fluoro-5-trifluoromethylpyridine (**47**) and 2-amino-4-iodopyridine (**48**) under nucleophile ionization and dual ionization conditions (Scheme 4C). Unsurprisingly given its high electrophilicity, complete selectivity for **47** was observed when using sodium methyl-4-mercaptobenzenethiolate (ArSNa) (**49**) (Reaction 1).[2b] Remarkably, when methyl 4-mercaptobenzoate (ArSH) (**24**) is used, the selectivity profile flips forming **27** exclusively (Reaction 2). Although Reaction 1 shows that **47** is significantly more electrophilic than **48**, Reaction 2 demonstrates how proton transfer remarkably enhances the electrophilicity of 4-halopyridines beyond even highly electrophilic 2-halopyridines.[2b] These experiments paired with those shown in Tables 2/3 help showcase valuable differences in chemoselectivity that could be exploited in complex molecules containing multiple sites of halogenation.

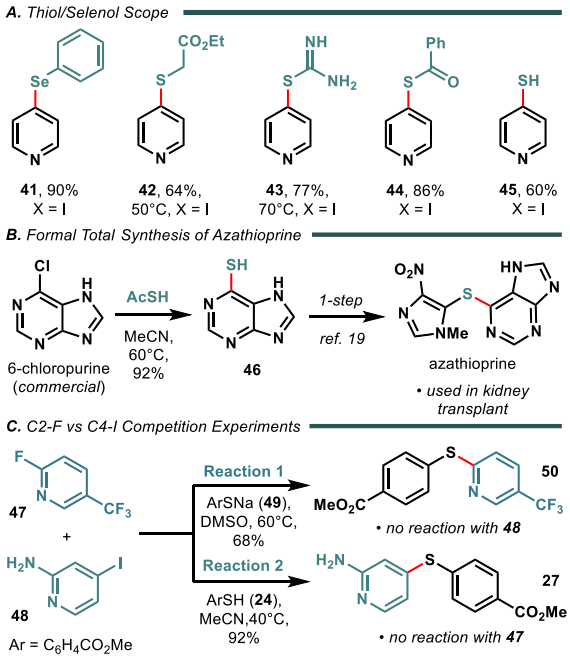

Scheme 4. A. Thiol/selenol scope. X represents the leaving group used. **B.** Formal total synthesis of azathioprine. **C.** Competition experiments between **47** and **48**.

After establishing the reaction scope, we performed reaction progress kinetic analysis (RPKA) to validate our mechanistic hypothesis (Scheme 5).[20] The reaction between methyl 4-mercaptobenzoate (**24**) and 2-amino-4-iodopyridine (**48**) in DMSO at varying equivalents and temperatures was monitored using Fourier Transform Infrared Resonance (FT-IR) Spectroscopy. These data were then modeled to Reaction Lab software which fit rate-limiting proton transfer (RLPT) pre-equilibrium (Keq = 10^{-6}) as the initial step.[21] Of note, fitting initial addition of **24** prior to proton transfer did not fit our rate data (Figure S13-16). The resulting pyridinium thiolate ion pair **A** then forms **27-HI**, at three orders of magnitude faster rate than proton transfer. Initial RLPT pre-equilibrium is unique for several reasons, most notably because addition is the archetypal RDS for S_NAr reactions. Additionally, while a RLPT has been characterized in some S_NAr reactions with amine nucleophiles, proton transfer takes place after an initial addition step, thus providing no electrophile activation.[11,20b] This finding also helps explain how more acidic/less nucleophilic thiols (like methyl 4-mercaptobenzoate) proceed with increased rate compared to less acidic/more nucleophilic thiols, and analogously how less basic haloheterocycles (pKa<2) struggle to form product.

Although RPKA resolved the initial proton transfer step, the subsequent steps to product could not be determined experimentally due to thermodynamic pre-equilibrium control from the RLPT step. While an addition step was assumed to occur next, it was unclear if this followed a classical stepwise elimination pathway (Scheme S2) or was concerted (cS_NAr). Of note, cS_NAr is a rapidly growing class of S_NAr reactions where strong electron withdrawing and good leaving groups that stabilize the classical Meisenheimer complex are superfluous.[22] In turn, computational studies were undertaken to elucidate the final steps of the mechanism. Following DFT calculations at the B3LYP-D3 level of theory, a two-coordinate potential energy surface (PES) scan was performed (Figure S17).[23] This was done to identify saddle point(s) along the PES which could serve as transition state (TS) candidates. This scan identified a single candidate which was confirmed as the TS (**B**) for the addition step by intrinsic reaction coordinate (IRC) calculations (Scheme 5). All attempts to locate a ground state sigma-complex or a second TS corresponding to a stepwise pathway failed. These results support an asynchronous cS_NAr, consistent with other examples in the literature.[22] Additionally, in line with our RPKA, the relatively low barrier (13.2 kcal/mol) for this TS reinforces thermodynamic control of the reaction rate by proton transfer pre-equilibrium.

Given this reaction's divergence from traditional S_NAr reactions, we have termed this mechanistic pathway proton transfer dual ionization (PTDI) S_NAr (Scheme 5). Like nucleophile ionization, anion formation proceeds the addition step which by contrast is not the RDS.[2a,g] For electrophile ionization, proton transfer is often rate determining but diverges from PTDI in that RLPT follows the addition.[21] PTDI capitalizes on the advantages of both nucleophile and electrophile ionization present in disparate S_NAr reactions. In theory, other types of appropriately matched nucleophiles and electrophiles could participate in S_NAr reactions

following a similar mechanism. Efforts to uncover such reactions are currently underway within our group.

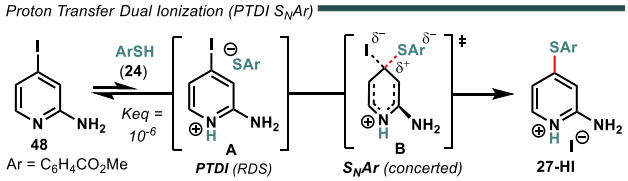

Scheme 5. Proposed reaction mechanism supported by RPKA and computational studies.

Conclusion

In conclusion, efforts to develop general photochemical conditions for C-S coupling uncovered a mild, light, transition metal and exogenous base free coupling between thiols and halogenated heterocycles. Control and ^{1}H NMR titration experiments identified substrate structural requirements and preliminary mechanistic features that guided substrate scope evaluation. 40 products derived from thiols and halogenated heterocycles could be generated cleanly at ambient temperature or with mild heating. RPKA and computation supports a unique mechanism involving dual nucleophile and electrophile ionization through a RLPT event, followed by cS$_N$Ar. This transformation compliments modern synthetic approaches to aryl thioethers and motivates additional research evaluating PTDI as a general activation mode when coupling nucleophiles and electrophiles.

AUTHOR INFORMATION

Corresponding Author

Christian R. Zwick III - *AbbVie Process Research & Development, 1401 N. Sheridan Road, North Chicago, Illinois 60064, United States*; https://orcid.org/0000-0002-8640-6727, Email: christian.zwick@abbvie.com,

Authors

Jeremy J. Henle - *AbbVie Process Research & Development, 1401 N. Sheridan Road, North Chicago, Illinois 60064, United States*

Shashank Shekhar - *AbbVie Process Research & Development, 1401 N. Sheridan Road, North Chicago, Illinois 60064, United States*

Cassie Yang - *AbbVie Process Research & Development, 1401 N. Sheridan Road, North Chicago, Illinois 60064, United States*

Yong Zhou - *Janssen Research & Development, 335 Phoenixville Pike, Malvern, Pennsylvania, 19355, United States*

Amanda L. Wall - *AbbVie Process Research & Development, 1401 N. Sheridan Road, North Chicago, Illinois 60064, United States*

Rodger F. Henry - *AbbVie Process Research & Development, 1401 N. Sheridan Road, North Chicago, Illinois 60064, United States*

Author Contributions

This work was conceived and directed by C. R. Zwick III. The manuscript was written by C. R. Zwick III, J. J. Henle and S. Shekhar. C. R. Zwick III performed laboratory experiments. Y. Zhou analyzed FT-IR data and performed MVDA. S. Shekhar performed kinetic modeling in Reaction Lab. J. J. Henle performed computational experiments. Analytical data was collected and analyzed by C. R. Zwick III, C. Yang, and A. L. Wall. X-ray crystallographic analysis was performed by R. F. Henry. The supporting information was prepared by all authors.

Funding Sources

All authors are or were employees of AbbVie who sponsored and funded this study.

Notes

The authors declare no competing financial interest. Yong Zhou has no conflict of interest.

ACKNOWLEDGMENT

Michael C. Haibach, Ryan M. Phelan, Jianguo Ji and Aleksandra E. Holownia provided useful discussion involving manuscript preparation and experimental suggestions.

REFERENCES

1. (*a*) M. Feng, B. Tang, S. H. Liang, X. Jiang, *Curr Top Med Chem*., 2016, **16**, 1200—1216. (*b*) M. Kazemi, S. Sajjadifar, A. Aydi, M. M. Heydari, *J. Med. Chem. Sci.*, 2018, **1**, 1—4. (*c*) E. A. Ilardi, E. Vitaku, J. T. Njardarson, *J. Med. Chem.*, 2014, **57**, 2832—2842. (*d*) B. R. Beno, K.-S. Yeung, M. D. Bartberger, L. D. Pennington, N. A. Meanwell, *J. Med. Chem.*, 2015, **11**, 4383—4438. (*e*) D. G. Brown, J. Boström, *J. Med. Chem.*, 2016, **59**, 4443—4458.

2. (*a*) J. P. Bunnett, R. E. Zahler, *Chem. Rev.*, 1951, **49**, 273—412. (*b*) J. A. Joule, K. Mills, *Heterocyclic Chemistry*, Wiley, Chichester, 2010. (*c*) Y.-J. Cherng, *Tetrahedron*, 2002, **58**, 4931—4935. (*d*) C. C. Eichman, J. P. Stambuli, *Molecules*, 2011, **16**, 590—608. (*e*) B. Liu, C.-H. Lim, G. M. Miyake, *Synlett*, 2018, **29**, 2449—2455. (*f*) B. Liu, C.-H. Lim, G. M. Miyake, *J. Am. Chem. Soc.*, 2017, **139**, 13616—13619. (*g*) Y. Ishihara, A. Montero, P. S. Baran, *The Portable Chemist's Consultant A Survival Guide for Discovery, Process, and Radiolabeling*, The Scripps Research Institute, La Jolla, 2016. (*h*) B. A. Hopkins, B. Zavesky, D. White, *J. Org. Chem.* 2022, **87**, 7547—7550. (*i*) R. A. Saikia,, N. Hazarika, N. Biswakarma, R. C. Deka, A. J. Thakur, *Org. Biomol. Chem.*, 2022, **20**, 3890—3896. (*j*) M. C. Kozlowski, *Org. Lett.* 2022, **24**, 7247—7249.

3. (*a*) E. G. Moschetta, S. M. Richter, S. J. Wittenberger, *ChemPhotoChem*, 2017, **1**, 539—543. (*b*) K. C. Harper, E. G. Moschetta, S. V. Bordawekar, S. J. Wittenberger, *ACS Cent. Sci.*, 2019, **5**, 109—115. (*c*) K. C. Harper, E.-X. Zhang, Z.-Q. Liu, T. Grieme, T. B. Towne, D. J. Mack, J. Griffin, S.-Y. Zheng, N.-N. Zhang, S. Gangula, J.-L. Yuan, R. Miller, P.-Z. Huang, J. Gage, M. Diwan, Y.-Y. Ku. *Org. Process Res. Dev.*, 2022, **26**, 404—412. (*d*) A. W. Dombrowski, N. J. Gesmundo, A. L. Aguirre, K. A. Sarris, J. M. Young, A. R. Bogdan, M. C. Martin, S. Gedeon, Y. Wang, *ACS Med. Chem. Lett.*, 2020, **11**, 597—604. (*e*) N. Borlinghaus, B. Schönfeld, S. Heitz, J. Klee, S. Vukelić, W. M. Braje, A. Jolit, *J. Org. Chem.*, 2021, **86**, 16535—16547. (*f*) E. C. Swift, S. Shekhar, B. J. Kotecki, *Org. Lett.*, 2020, **22**, 5363—5368.

4. (*a*) Y. Wang, I. Haight, R. Gupta, A. Vasudevan, *J. Med. Chem.*, 2021, **64**, 17115—14122. (*b*) A. W. Dombrowski, A. L. Aguirre, A. Shrestha, K. A. Sarris, Y. Wang, *J. Org. Chem.*, 2022, **87**, 1880—1897.

5. K. D. Collins, F. Glorius, *Nat. Chem.*, 2013, **5**, 597—601.

6. E. B. Corcoran, M. T. Pirnot, S. Lin, S. D. Dreher, D. A. DiRocco, I. W. Davies, S. L. Buchwald, D. W. C. MacMillan, *Science*, 2016, **353**, 279—283.

7. (*a*) N. Kerru, L. Gummidi, S. Maddila, K. K. Gangu, S. B. Jonnalagadda, *Molecules*, 2020, **25**, 1909—1951. (*b*) J. L. Henderson, S. M. McDermott, S. L. Buchwald, *Org. Lett.*, 2010, **12**,

4438—4441. (*c*) M. A. Düfert, K. L. Billingsley, S. L. Buchwald, *J. Am. Chem. Soc.*, 2013, **135**, 12877—12885.
8. (*a*) I. M. Kolthoff, M. K. Chantooni Jr., S. Bhowmik, *J. Am. Chem. Soc.*, 1968, **90**, 23—28. (*b*) F. G. Bordwell, *Acc. Chem. Res.*, 1988, **21**, 456—463.
9. Y. Qin, R. Sun, N. P. Gianoulis, D. G. Nocera, *J. Am. Chem. Soc.*, 2021, **143**, 2005—2015.
10. (*a*) J. Ma, S. Chen, P. Bellotti, R. Guo, F. Schäffer, A. Heusler, X. Zhang, C. Daniliuc, M. K. Brown, K. N. Houk, F. Glorius, *Science*, 2021, **371**, 1338—1345. (*b*) H. Fuse, U. Irie, M. Fuki, Y. Kobori, K. Kato, A. Yamakata, M. Higashi, H. Mitsunuma, *J. Am. Chem. Soc.*, 2022, ASAP, doi: 10.1021. (*c*) D. Moser, Y. Duan, F. Wang, Y. Ma, M. J. O'Neill, J. Cornella, *Angew. Chem. Int. Ed.*, 2018, **57**, 11035—11039. (*d*) J. Liu, M. J. Robins, *J. Am. Chem. Soc.*, 2007, **129**, 5962—5968. (*e*) P. S. Fier, S. Kim, R. D. Cohen, *J. Am. Chem. Soc.*, 2020, **142**, 8614—8618.
11. (*a*) A. Kinens, S. Balkaitis, E. Suna, *J. Org. Chem.*, 2018, **83**, 12449—12459. (*b*) M. Schlosser, F. Cottet, *Eur. J. Org. Chem.*, 2002, **2002**, 4181—4184. (*c*) B. T. Boyle, J. L. Koniarczyk, A. McNally, *Synlett*, 2021, **32**, 215—218. (*d*) J. H. Kim, T. Constantin, M. Simonetti, J. Llaveria, N. S. Sheikh, D. Leonori, *Nature*, 2021, **595**, 677—683. (*e*) J. Choi, G. Laudadio, E. Godineau, P. S. Baran, *J. Am. Chem. Soc.*, 2021, **143**, 11927—11993.
12. (*a*) F. G. Bordwell, D. L. Hughes, *J. Org. Chem.*, 1982, 47, 3223—3232. (*b*) Equilibrium pKa Table (DMSO Solvent and Reference), https://organicchemistrydata.org/hansreich/resources/pka/pka_data/pka-compilation-reich-bordwell.pdf, (accessed April 2022).
13. (*a*) R. A. Rossi, A. B. Pierini, A. B. Peñéñory, *Chem. Rev.*, 2003, **103**, 71—168. (*b*) A. J. Boyington, M.-L. Y. Riu, N. T. Jui, *J. Am. Chem. Soc.*, 2017, **139**, 6582—6585. (*c*) A. G. Myers, M. Movassaghi, B. Zheng, *Tetrahedron Lett.*, 1997, **38**, 6569—6572.
14. (a*)* S. J. Fussell, A. Luan, P. Peach, G. Scotney, *Tetrahedron Lett.*, 2012, **53**, 948—951. (*b*) R. Sarges, H. R. Howard, K. M. Donahue, W. M. Welch, D. W. Dominy, A. Weissman, B. K. Koe, J. Bordner, *J. Med. Chem.*, 1986, **29**, 8—19.
15. (*a*) K. M. Maloney, J. T. Kuethe, K. Linn, *Org. Lett.*, 2011, **13**, 102—105. (b) B. Sreedhar, P. S. Reddy, M. A. Reedy, *Synthesis*, 2009, **10**, 1732—1738.
16. (*a*) S. Roy, P. Phukan, *Tetrahedron Lett.*, 2015, **56**, 2426—2429. (*b*) X. Ma, L. Yu, C. Su, Y. Yang, H. Li, Q. Xu, *Adv. Syn. Catal.*, 2017, **359**, 1649—1655. (*c*) V. Magné, L. T. Ball, *Chem. Eur. J.*, 2019, **25**, 8903—8910. (*d*) S. Ziao, K. Xie, J. Qi, *Chinese J. Org. Chem.*, 2010, **28**, 1441—1443.
17. F. Jordan, Z. Kudzin, Z. Witczak, P. Hoops, *J. Org. Chem.*, 1986, **51**, 571—573.
18. (*a*) G. C. Llyod-Jones, J. D. Moseley, J. S. Renny, *Synthesis*, 2008, **5**, 661—689. (*b*) A. Rostami, A. Rostami, N. Iranpoor, M. A. Zolfigol, *Tetrahedron Lett.* 2016, **57**, 192—195. (*c*) L. Testaferri, M. Tiecco, M. Tingoli, D. Chianelli, M. Montanucci, *Synthesis*, 1983, **9**, 751—755.
19. *CN Pat.*, CN101486681, 2009.
20. a) D. G. Blackmond, *Angew. Chem. Int. Ed.*, 2005, **44**, 4302—4320. b) I. W. Ashworth, L. Frodsham, P. Moore, T. O. Ronson, *J. Org. Chem.*, 2022, **87**, 2111—2119.
21. (a) J. T. Bowler, F. M. Wong, S. Gronert, J. R. Keeffe, W. Wu., *Org. Biomol. Chem.*, 2014, **12**, 6175—6180. (*b*) Dynochem build 2.0.49b614 (Data 1.0); Scale-up suite: www.scale-up.com.
22. (*a*) E. E. Kwam, Y. Zeng, H. A. Besser, E. N. Jacobsen, *Nat. Chem.*, 2018, **10**, 917—923. (*b*) S. Rohrbach, A. J. Smith, J. H. Pang, D. L. Poole, T. Tuttle, S. Chiba, J. A. Murphy, *Angew. Chem. Int. Ed.*, 2019, **58**, 16368—16388.
23. A. D. Becke, *J. Chem. Phys.*, 1993, **98**, 1372—1377.

SYNOPSIS TOC (Word Style "SN_Synopsis_TOC")

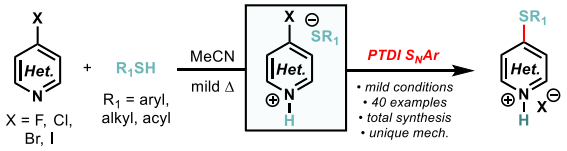

Insert Table of Contents artwork here